Published in final edited form as:
Biosens Bioelectron. 2010 November 15; 26(3): 964–969. doi:10.1016/j.bios.2010.08.004.

Label Free Detection of White Spot Syndrome Virus Using Lead Magnesium Niobate-Lead Titanate Piezoelectric Microcantilever Sensors

Joseph Capobianco,
Department of Materials Science and Engineering, Drexel University, Philadelphia, PA, 19104

Wei-Heng Shih,
Department of Materials Science and Engineering, Drexel University, Philadelphia, PA, 19104

Jiann-Horng Leu*,
College of Life Science, National Taiwan University, Taipei, Taiwan

Grace Chu-Fang Lo, and
College of Life Science, National Taiwan University, Taipei, Taiwan

Wan Y. Shih
School of Biomedical Engineering, Science, and Health Systems, Drexel University, Philadelphia, PA 19104

Abstract

We have investigated rapid, label free detection of white spot syndrome virus (WSSV) using the first longitudinal extension resonance peak of five lead-magnesium niobate-lead titanate (PMN-PT) piezoelectric microcantilever sensors (PEMS) 1050-700 μm long and 850-485 μm wide constructed from 8 μm thick PMN-PT freestanding films. The PMN-PT PEMS were encapsulated with a 3-mercaptopropltrimethoxysilane (MPS) insulation layer and further coated with anti-VP28 and anti-VP664 antibodies to target the WSSV virions and nucleocapsids, respectively. By inserting the antibody-coated PEMS in a flowing virion or nucleocapsid suspension, label-free detection of the virions and nucleocapsids were respectively achieved by monitoring the PEMS resonance frequency shift. We showed that positive label-free detection of both the virion and the nucleocapsid could be achieved at a concentration of 100 virions (nucleocapsids)/ml or 10 virions (nucleocapsids)/100μl, comparable to the detection sensitivity of polymerase chain reaction (PCR). However, in contrast to PCR, PEMS detection was label-free, in-situ and rapid (less than 30 min), potentially requiring minimal or no sample preparation.

Keywords

Virus; detection; piezoelectric; cantilever; sensor; detection

*Current Address: Center for Marine Bioenviroment and Biotechnology, National Taiwan Ocean University, No. 2, Pei-Ning Road, Keelung 20224, Taiwan, ROC

1. Introduction

White spot syndrome virus (WSSV) is a devastating shrimp viral pathogen that causes serious economic losses to shrimp aquaculture industry globally. This virus has a wide host range, attacking shrimp, crabs, lobster as well as many other crustaceans (Corbel, et al., 2001; Wang, et al. 1996; Lo, et al. 2006; Flegel, 2006), but the penaeid shrimp are most vulnerable to WSSV infection. In shrimp farms, WSSV infection causes up to 100% mortality within three to ten days following the first signs of infection (Lightner 1996). These clinical signs include a sudden reduction in food consumption, lethargy, loose cuticle, reddish discoloration, and the presence of white spots in the shrimp cuticle (Chou et al. 1995; Wang et al. 1995; Lightner 1996). Diagnosis for WSSV infection based on the gross signs of diseased shrimp is not practical for shrimp farming practices, as these clinical signs are not the pathonognomic characters only specific to WSSV infection, and the shrimp exhibiting these signs are at late stage of WSSV infection, indicating the outbreak of disease has occurred and preventive measures are too late. Therefore, it is necessary to develop a diagnostic method that can detect WSSV at low level or at early stage of infection. Various WSSV diagnostic methods have been developed, including polymerase chain reaction (PCR) (Takahashi et al. 1996; Lo et al. 1996; Kimura et al. 1996), *in situ* hybridization (Durand et al. 1996; Chang et al. 1996; Wongteerasupaya et al. 1996), histological observation of sectioned tissue (Wongteerasupaya et al. 1995; Wang et al. 1997), and immunological-based methods (Poulos et al. 2001; Anil e al. 2002; Liu et al. 2002).

Currently, PCR is the most widely used method for WSSV detection, as it provides high specificity and sensitivity. Most of the commercial kits for WSSV diagnosis are based on this technology, and many different protocols have been developed. The Taqman real-time PCR was the most sensitive method, which could detect WSSV of 4-5 copies per reaction (Durand and Lightner 2002; Sritunyalucksana et al. 2006). The nested two-step PCR methods detected 50-100 copies of WSSV, whereas the one-step PCR could detect 1000 copies (Sritunyalucksana et al. 2006). Immunological-based diagnostic methods have been investigated or developed including immunodot test (Anil e al. 2002) and antigen-capture ELISA (Ac-ELISA) test (Liu et al. 2002). Their detection limits are about 400-500 pg of WSSV protein, and are comparable to one-step PCR. The immunological-based kit using lateral flow chromatographical detection strips is now commercially available (Shrimple Test Kits). The sensitivity is not high (> 10,000 viral particles), but the kit is cheap, easy to use, and do not need the use of specific instrument. Therefore, it is suitable for use at pond-side by farmers to verify disease outbreaks. Although the sensitivity of immunological-based detection method can only reach the limit of one-step PCR, the sample preparation processes for immunological detection is simple, time-saving and without the need of expensive instruments. Therefore, techniques based on antibody-antigen reaction are still continuously developed for WSSV detection; for example, the reverse passive latex agglutination assay (Okuruma et al. 2005) and surface plasmon resonance (SPR) techniques (Lei et al. 2008).

Piezoelectric microcantilever sensors (PEMS) are a new type of sensors that consist of a highly piezoelectric layer such as lead zirconate titanate (PZT) or lead magnesium niobate-lead titanate, $(PbMg_{1/3}Nb_{2/3}O_3)_{0.63}$-$(PbTiO_3)_{0.37}$ (PMN-PT) (Shih, et al. 2006) bonded to a nonpiezoelectric layer such as glass, tin, or copper. Receptors or antibodies specific to target molecules can be immobilized on the PEMS surface. Binding of target molecules to the PEMS surface shifts the PEMS resonance frequency. Real-time, in-situ, label-free detection of the target molecules can be achieved by monitoring the PEMS resonance frequency shift using simple electrical means. Compared to silicon microcantilevers, PEMS do not require complex optical components, and their quality factor--which is defined as the ratio of the peak frequency over the width at half the peak height--can remain high when submerged in a

liquid medium (Yi, et al. 2003). PEMS can be electrically insulated using a silane base coating (Capobianco, et al. 2006; Capobianco, et al. 2007; Capobianco, et al. 2008) or paralyene (Hwang, et al. 2004) for in-liquid detection. PEMS have successfully been used in rapid, label-free, and sensitive detection of bacteria (Capobianco et al. 2006; Zhu, et al. 2007a; Zhu, et al. 2007b) in phosphate buffer saline solution (PBS), human epidermal growth factor receptor 2 (Her2) in PBS with a background of Bovine serum albumin (BSA) (Capobianco et al. 2007, Capobianco et al. 2008), and spores in PBS and in water (McGovern, et al. 2007; McGovern, et al. 2008).

Although PEMS use electrical means for detection and silicon microcantilevers use optical means or piezoresistivity for detection, PEMS resonator sensors (Yi et al. 2002) and silicon microcantilever (Chen et al., 1995)/silicon nanocantilever (Gupta, et al. 2006) resonator sensors have long been regarded as the same type of sensors in that (1) both use flexural-mode resonance peaks for detection and (2) both are mass sensors, i.e., binding of target antigen to the receptors on the sensor surface increases the sensor mass that in turn decreases the sensor resonance frequency. Interestingly, our recent studies and others' on PZT PEMS showed that PZT PEMS detection resonance frequency shift was more than 100 times larger than could be accounted for by the mass change (Lee, J. H., 2004a, 2004b, 2005, Zhu et al. 2007a, Zhu et al. 2007b). These results clearly set PEMS apart from mass sensors. In addition, highly piezoelectric materials such as PMN-PT are prone to polarization orientation change under stress or under an electric field. Studies on PMN-PT PEMS showed that the flexural-mode detection resonance frequency shift of PMN-PT PEMS was a result of the elastic modulus change due to the stress-induced polarization orientation change in the PMN-PT layer by the binding of the target analyte to the PEMS surface (Zhu et al. 2008; Shih et al. 2008). Due to this elastic modulus changeme chanism, the detection sensitivity of a PMN-PT PEMS was amplified 300 times (Zhu et al. 2008; Shih et al. 2008) higher than could be accounted for by mass loading alone. Zhu et al. (2008a and 2008b) further showed that PMN-PT PEMS could also exhibit high-frequency non-flexural resonance modes such as longitudinal extension modes that nonpiezoelectric microcantilevers such as silicon-based microcantilevers lack as a result of the high piezoelectricity of the piezoelectric layer. In view of a PMN-PT PEMS amplified detection resonance frequency shift through its elastic modulus change mechanism and that it also offers higher-frequency non-flexural mode resonance peaks, it is of interest to investigate PMN-PT PEMS for WSSV detection.

The purpose of this study is to investigate the label-free detection of WSSV using the first longitudinal mode resonance peak of a PMN-PT PEMS consisted of 8 μm thick PMN-PT freestanding sheet bonded with a 2 μm thick copper layer that exhibits elastic-modulus-change induced detection enhancement. We carried out direct detection of virions and the nucleocapsides by targeting an envelope protein, VP28 and the nucleocapsid protein, VP664, respectively. For comparison we also removed the envelope of the viruses and detected the isolated nucleocapsids by targeting the nucleocapsid protein VP664.

2. Experimental

a. PMN-PT PEMS fabrication

Five PMN-PT/Cu PEMS were used in this study. They were constructed from PMN-PT freestanding sheets of 8 μm in thickness. A 150 nm thick gold layer with a 15-30 nm thick chromium bonding layer was first deposited on one side of the PMN-PT freestanding sheet by evaporation (E-gun Evaporator, Semicore Equipment, Livermore, CA) to serve as an electrode for plating. A 2-μm thick copper layer was electroplated on the gold surface at a rate of 500 nm/min as the nonpiezoelectric layer using a plating solution of copper sulfate. After copper plating, a 150-nm thick gold was evaporated on both sides of the sheet. The

PMN-PT/Cu bilayer was then embedded in wax and cut to the cantilever shape with a wire saw (Princeton Scientific Precision, Princeton, NJ). After attaching the wires to the top and bottom electrodes using conductive glue (XCE 3104XL, Emerson and Cuming Company, Billerica, MA), the PMN-PT/Cu strips were finally glued to a glass substrate to form the microcantilevers (Shih, et al., 2006, Zhu et al. 2008a and Zhu et al. 2008b).

b. Electrical Insulation of PEMS

The PEMS was first soaked in a diluted (1:100 in water) piranha solution (two parts of 98% sulfuric acid (Fisher, Fair Lawn, NJ) with one part of 30% hydrogen peroxide (FisherBiotech, Fair Lawn, NJ) at 20°C for 1 min to clean the gold surfaces. The PEMS was then submerged 0.1 mM solution of 3-mercaptopropltrimethoxysilane (MPS) in ethanol (Tremont, et al. 2000) covered with parafilm to prevent ethanol evaporation for 30 minutes. The PEMS was then dried in a vacuum-oven (Model 1400E, VWR International) at 762 mm Hg overnight followed by soaking in a 1 vol% MPS solution in ethanol titrated to a pH 4.5 with acetic acid and covered with parafilm for 36 hours with the solution being changed every 12 hours. They then dried overnight in a vacuum-oven (Model 1400E, VWR International) at 762 mm Hg and rinsed with ethanol. Based upon our previous results we estimated the thickness of the MPS layer to about 250 nm (Capobianco, 2007, Capobianco, 2008).

c. Purifications of WSSV Virions and Nucleocapsids

The WSSV in this study was originated from WSSV-infected *P. monodon* collected in Taiwan in 1994 (Wang et al. 1995; GenBank accession number AF440570), and then propagated in specific pathogen-free *L. vannamei* to prepare the virus stock (Wang et al. 2007). The inocula were prepared from the stock and injected into healthy crayfish *P. clarkii* according to Tsai et al. (2004). At one week post infection, the moribund crayfish were collected and the virions were purified from the crayfish tissues according to the methods developed by Xie et al. (2005). The OD_{600} value of purified WSSV virions was determined by using a spectrophotometer and the concentration of the corresponding virions was then calculated using the formula established by Zhou et al. (2007). To purify the WSSV nucleocapsids, a known amount of purified WSSV virions were treated with 1% Triton X-100 in TMN buffer (20 mM Tris-HCl, 150 mM NaCl, 2 mM MgCl2, pH 7.5) for 30 min at room temperature with occasional shaking. Subsequently, the samples were centrifuged at 20,000g for 20 min at 4°C, rinsed with water and then resuspended with TMN buffer. We assumed that the amount of purified nucleocapsids equal to that of the input virions.

d. Antibody Purification

Polyclonal anti-VP28 and anti-VP664 antibodies were raised by injecting recombinant VP28 and VP664 in rabbits. After collecting the sera from the rabbits, ImmunoPure (Protein A) IgG Purification Kit (Pierce Biotechnology) was used to purify the anti-VP28 and anti-VP664 antibodies from the corresponding rabbit antisera according to the supplier's protocol. The purified antibodies were desalted and concentrated in phosphate-buffered saline through an Amicon Ultra–15 centrifugal filter device (Millipore). Subsequently, the antibodies were quantified using the Bradford method (BioRad), and freeze-dried for long term storage until use.

e. Antibody immobilization

A heterobifunctional crosslinker, Sulfosuccinimidyl 4-N-maleimidomethyl cyclohexane-1-carboxylate (sulfo-SMCC) was used to tether the purified VP28 or VP664 antibodies to the PEMS surface. The antibody was first covalently bonded to sulfo-SMCC by using 1 ml solution containing 1 μM antibody and 80 μM sulfo-SMCC for 2 hr at 4°C for the NHS-

ester of the sulfo-SMCC to react with a primary amine of the antibody to form a peptide bond. Unreacted sulfo-SMCC molecules were then removed by repeated microcentrifugation at 6000 RPM with a 10kD filter (Millipore) three times. The MPS-coated PEMS was then soaked in the sulfo-SMCC-linked antibody solution with 5 mM ethylenediaminetetraacetic acid (EDTA) (Pierce) for 2 hr to immobilize the antibody on the MPS coating surface via the reaction of the maleimide of the sulfo-SMCC with the sulfhydryl of the MPS. Following the antibody immobilization the PEMS was submerged in a 30 mg/ml BSA solution in PBS for non-specific binding prevention (Capobianco et al. 2007, Capobianco et al. 2008). At this point, the PEMS may be stored in a humidified container in a refrigerator for up to several days before being used for detection. A total of 5 PEMS were used throughout this study.

3. Results and Discussions

a. PEMS resonance spectra

Figure 1(a) shows an optical micrograph of a PEMS 715 μm long and 485 μm wide viewed from the gold side. For a PEMS with a thickness h, length L, and a sound velocity c, the first longitudinal extension mode is $c/4L$ (Capobianco, 2009). On the other hand, the resonance frequency of a flexural mode is proportional to ch/L^2 (Yi, et al. 2002). Therefore, the resonance frequency of a longitudinal mode could be higher than that of a flexural mode by a factor on the order of the aspect ratio, L/h. For a PEMS 715 μm long and 10 μm thick (8 μm PMN-PT and 2 μm copper), L/h was about 71. We show the typical PEMS phase angle-versus-frequency resonance spectra in Fig. 1(b). The dashed and solid lines represent the spectra in air and in PBS, respectively. As can be seen, the first longitudinal peak was at around 1000 kHz, which was much higher than the flexural peaks as marked by arrows. In addition, the longitudinal peak can better withstand liquid damping than flexural modes. As can be seen in Fig. 1(b), the first longitudinal extension mode retained much of the peak height with a Q value of about 25 in PBS.

b. Flow system and WSSV detection

For detection, the PEMS were vertically inserted in the center of a home-made polycarbonate flow channel with its major faces parallel to the flow as shown in the photograph in Fig. 2(a) and the schematic in Fig. 2(b). The detection chamber was 18.5 mm long, 3.5 mm wide, and 5.5 mm deep (volume = 356 μl) driven with a peristaltic pump (model 77120-62, Cole-Parmer's Master Flex, Vernon Hills, IL). All experiments were carried out at a flow rate of 1 ml/min corresponding to an average flow velocity of 1.4 mm/s. A stock virus (nucleocapsid) suspension (10^9 virus/ml) was diluted to suspensions of 10^8 to 50 viruses/ml using 1:10 serial dilution. Before each detection, we first flowed PBS to allow the PEMS to equilibrate with the PBS at room temperature until the resonance frequency of the PEMS become stable, i.e., with no more than 100 Hz shift in 30 min. A similar stabilization procedure has been employed in other resonator detection systems (Sakti, et al. 1999). Once the PEMS had stabilized, 10 minutes of background monitoring was performed for t = -10 to 0 min. At t = 0 minutes, 60 μl of a concentrated suspension of viruses or nucleocapsids in PBS was spiked in the reservoir (see Fig. 2(a)). A total liquid volume of 6 ml was used, most of which resided in the reservoir and the long tubes connecting the detection chamber and the reservoir. Injecting 60 μl of a suspension of 1×10^7-5×10^3 viruses/ml in the reservoir yielded concentrations of 10^5-50 virions (nucleocapsids)/ml in the flow system.

According to Shih et al. (2008), the relative resonance frequency shift, $\Delta f/f$, was independent of the length and width of the PEMS and was only proportional to the surface stress, s, resulted from antigen binding and inversely proportional to the thickness, h, of the

device as $\Delta f/f \propto s/h$ where f was the initial resonance frequency and Δf the resonance frequency shift defined as the difference of the resonance frequency at time, t, and the initial resonance frequency at t = 0. For the same antigen-antibody pair, the surface stress, *s*, would only depend on the concentration and for the same antigen concentration, *s* would only depend on the antibody-antigen pair used. As all current PEMS had the same thickness but varying lengths, we plot Δf/f versus time for the direct detection of the viruses with anti-VP28 antibody coated PEMS for concentrations ranging from 10^5-50 viruses/ml is plotted in Fig 3(a). The detection Δf/f versus time for nucleocapsid detection using anti-VP664 coated PEMS at concentrations 10^5 to 50 nucleocapsids/ml is plotted in Fig. 3(b).

Note in all the detection events shown in Figs. 3(a) and 3(b), there was no discernable artificial signal arising from the spiking events. In addition, there was a delay in the onset of detection until about t = 10 min. We attributed the delay in detection and the absence of an artificial signal from spiking to the following preventive measures we had taken: (1) By spiking in a reservoir away from the detection channel to minimize the possibility of artificial spiking signal and to allow more time for mixing, (2) by spiking near the top of the reservoir while keeping the opening of the tubes at the bottom of the reservoir and by using a long (>100 cm) tube connecting the reservoir to the inlet of the detection channel to delay the reach of the virions and nucleocapsides to the detection channel, and (3) by keeping the PEMS near the top of the detection channel while the inlet and outlet were at the bottom of the detection chamber (Fig. 2(b)) to further prevent the virions and nucleocapsides from reaching the PEMS before they were well mixed with the liquid.

From Figs. 3(a) and 3(b), one can see that starting around t = 10 min, Δf/f decreased with time for a given virion (nucleocapsid) concentration, signaling binding of the virions (nucleocapsids) to the antibody on PEMS surface. For all concentrations larger or equal to 100 virions (nucleocapsids)/ml, the |Δf/f| at t = 60 min was larger than the noise--the fluctuations of the Δf/f with time—which was about $5\text{-}8\times10^{-5}$ (corresponding to a Δf of 60-80 Hz) as discussed below. In contrast, at 50 virions(nucleocapsids)/ml the |Δf/f| at t = 60 min was smaller than the noise, indicating no positive detection of either the virions or nucleocapsids at this concentrations and the concentration sensitivity for both the virions and the nucleocapsids was 100 virions (nucleocapsids)/ml.

In Tables I, and II we listed the values of f, $\Delta f_{30}/f$ and $\Delta f_{60}/f$ at various virion and nucleocapsid concentrations where Δf_{30} and Δf_{60} were the resonance frequency shift averaged over t = 29-31 min and that averaged over t = 55-60 min, respectively. Note that for each Δf/f, the number after the "±" indicated the noise—half the band width of the fluctuations of Δf/f with time. Although we obtained nonzero values for $\Delta f_{30}/f$ and $\Delta f_{60}/f$ at 50 virions/ml and at 50 nucleocapsids/ml, these values were smaller than the noise of Δf/f with time, indicating that they were insignificant. As a result, we recorded zero for the $\Delta f_{30}/f$ and $\Delta f_{60}/f$ for both 50 virions/ml and 50 nucleocapsids/ml in Table I and II.

To better illustrate the concentration dependence, we plot $\Delta f_{30}/f$ and $\Delta f_{60}/f$ versus concentration for both virions and nucleocapsids in Fig. 4. As can be seen, both $\Delta f_{30}/f$ and $\Delta f_{60}/f$ increased with an increasing concentration for both virion and nucleocapsid. Note that even though both virions and nucleocapsids exhibited a concentration sensitivity of 100 virions/ml, the average frequency shift Δf/f was larger for the nucleocapsid than for the virion for every concentration and the difference was larger at time = 60 min than at time = 30 min, indicating that the binding of anti-VP664 to the nucleocapsid was stronger than that of anti-VP28 to the virion. The detailed comparison between the resonance frequency shifts for the virions and those for the nucleocapsids are shown in Table III. These results compared well with the result of Tsai et al. (2004) where the binding of anti-VP664 to the nucleocapsid and that of the anti-Vp28 to the virion were examined using transmission

electron microscopy (TEM). The TEM images showed that there were about 12 anti-VP28 coated gold particles bound to each virion and 21 anti-VP664 coated gold particles to each nucleocapsid indicating that binding of anti-VP664 to a nucleocapsid was stronger than that of anti-Vp28 to a virion, in agreement with the current detection result that at the same concentration, the Δf/f for detection of nucleocapsids was higher than that of detection of virions.

Note that although we injected a more concentrated suspension (e.g. 1×10^5 virions or nucleocapsids/ml) into a reservoir as a convenient way to achieve a sample of a desired concentration (e.g. 100 virions or nucleocapsids per ml) for detection in the current flow setup it does not imply that PEMS detection would always require injection of a more concentrated liquid in order to achieve positive detection. For example, detection without spiking can be accomplished by using two reservoirs instead of one: one containing the sample and the other PBS. Connection of detection cell to either the sample or to PBS is controlled by the valves. Such a flow system is commonly used in a BIAcore system or a quartz crystal microbalance (QCM). In a future study, we will examine PEMS detection with such a flow system. However, design and implementation of such of a flow system is not within the scope of this study.

The current flow rate of 1 ml/min corresponded to a flow velocity of $u = 1.4$ mm/s, which could be further increased to potentially increase the detection signal (McGovern et al. 2008). This is because an increase of flow velocity could circulate a larger liquid volume thus bringing more virions/nucleocapsids to pass the sensor surface per unit time, thereby increase the chance for the virions and nucleocapsids to bind to the sensor surface. On the other hand, an increase in flow rate can also increase the force impinging on a bound virion or ncleocapsid on the sensor surface leading to detachment of the bound virions/ nucleocapsids and potentially lead to decrease of detection signal. The flow induced impingement force can be estimated as $F = 1.7(6\pi\eta a)u$ (McGovern, et al. 2008) where $\eta = 1$ cP is the liquid viscosity, a the radius of the virion or nucleocapsid. As the largest dimension of either the virion or the nucleocapsid is on the order of 300 nm, we use $a = 150$ for overestimate and the impingement force for the bound virions or nucleocapsids at a flow velocity of 1.4 mm/s was estimated to be about 6 pN, which was still quite small compared to the 100 pN shown to unbind particles from the sensor surface that were bound by antibody-antigen binding (McGovern, et al. 2008). Based on this estimation, it is, therefore, likely that one can further increase detection signal and lower detection concentration limit by increasing the flow velocity, which will be examined in a future study and is not within the scope of the present study.

4. Conclusion

We have investigated rapid, label free detection of WSSV virions and nucleocapsids using the first longitudinal extension resonance peaks of 5 PMN-PT/Cu PEMS 1050-700 μm long and 850-485 μm wide. The PMN-PT/Cu PEMS were consisting of an 8-μm thick PMN-PT layer bonded with a 2-μm thick copper and further electrically insulated with a MPS coating. Detection of the virions and nucleocapsids was carried out by directly inserting the anti-VP28 and anti-VP664 coated PEMS at the center of the detection cell. The flowing suspension of 10^5 to 50 virions (nucleocapsids)/ml was created through a 100-fold dilution by spiking 60 μl of a 100-time concentrated suspension in a reservoir away from the detection channel to minimize the artificial spiking signal and prevent the PEMS from unwanted exposures to the un-mixed concentrate. Label-free detection of virions and nucleocapsids was achieved by monitoring the PEMS resonance frequency shift with time. We showed that both the virions and the nucleocapsids could be detected at a concentration 100 virions (nucleocapsids)/ml or 10 vrions (nucleocapsids)/100μl, comparable to the

detection sensitivity of PCR. However, in contrast to PCR, PEMS detection was label-free, in-situ, and rapid (less than 30 min), potentially requiring minimal or no sample preparation.

Acknowledgments

This work is supported in part by the National Institute of Health (NIH) under Grant No. R01 EB000720, and The Nanotechnology Institute, a University Grant program of the Commonwealth of Pennsylvania's Ben Franklin Technology Development Authority through Ben Franklin Technology Partners of Southeast Pennsylvania.

References

Anil TM, Shankar KM, Mohan CV. Dis Aquat Org. 2002; 51(1):67–75. [PubMed: 12240972]

Capobianco JA, Shih WY, Shih W-H. Rev Sci Instr. 2006; 77(12):125105.

Capobianco JA, Shih WY, Shih W-H. Rev Sci Instr. 2007; 78(4):046106.

Capobianco JA, Shih WY, Yuan Q-A, Adams GP, Shih W-H. Rev Sci Instr. 2008; 79(7):076101.

Capobianco, J. PhD thesis. Drexel University; Philadelphia, PA: 2009. Piezoelectric Microcantilever Serum Protein Detector; p. 10104

Chang PS, Lo CF, Wang YC, Kou GH. Dis Aquat Org. 1996; 27:131–139.

Chen GY, Thundat T, Wachter EA, Warmack RJ. J Appl Phys. 1995; 77(8):3618–3622.

Corbel V, Zuprizal, Shi Z, Huang C, Sumartono, Arcier JM, Bonami JR. Journal of Fish Diseases. 2001; 24(7):377–382.

Chou HY, Huang CY, Wang CH, Chiang HC, Lo CF. Dis Aquat Org. 1995; 23:165–173.

Durand S, Lightner DV, Nunan LM, Redman RM, Mari J, Monami JR. Dis Aquat Org. 1996; 27:59–66.

Durand SV, Lightner DV. J Fish Dis. 2002; 25:381–389.

Sritunyalucksana K, Srisala J, McColl K, Nielsen L, Flegel TW. Aquaculture. 2006; 255:95–104.

Flegel TW. Aquaculture. 2006; 258:1–33.

Gupta AK, Nair PR, Akin D, Ladisch MR, Broyles S, Alam MA, Bashir R. PNAS. 2006; 103(36): 13362–13367. [PubMed: 16938886]

Hwang KS, Lee JH, Park J, Yoon DS, Park JH, Kim TS. Lab Chip. 2004; 4(6):547–552. [PubMed: 15570363]

Kimura T, Yamano K, Nakano H, Momoyama K, Hiraoka M, Inouye K. Fish Pathol. 1996; 31:93–98.

Lightner, DV., editor. World Aquaculture Society. Baton Rouge, LA., USA: 1996. p. 305

Lee JH, Hwang KS, Park J, Yoon KH, Yoon DS, Kim TS. Biosens Bioelectron. 2005; 20:2157–2162. [PubMed: 15741091]

Lee JH, Kim TS, Yoon KH. Appl Phys Lett. 2004a; 84(16):3187–3189.

Lee JH, Yoon KH, Hwang KS, Park J, Ahn S, Kim TS. Biosens Bioelectron. 2004b; 20:269–275. [PubMed: 15308231]

Lei Y, Chen H, Dai H, Zeng Z, Lin Y, Zhou F, Pang D. Biosens Bioelectron. 2008; 23(7):1200–1207. [PubMed: 18023170]

Liu W, Wang YT, Tian DS, Yin ZC, Kwang J. Dis Aquat Org. 2002; 49(1):11–8. [PubMed: 12093036]

Lo CF, Ho CH, Peng SE, Chen CH, Hsu HC, Chiu YL, Chang CF, Liu KF, Su MS, Wang CH, Kou GH. Dis Aquat Org. 1996a; 27(3):215–225.

Lo CF, Leu JH, Ho CH, Chen CH, Peng SE, Chen YT, Chou CM, Yeh PY, Huang CJ, Chou HY, Wang CH, Kou GH. Dis Aquat Org. 1996b; 25:133–141.

Markidou A, Shih WY, Shih W-H. Rev Sci Ins. 2005; 76:064302.

McGovern J-P, Shih WY, Rest R, Purohit M, Pandya Y, Shih W-H. Analyst. 2008; 133(5):649–654. [PubMed: 18427687]

McGovern JP, Shih WY, Shih W-H. Analyst. 2007; 132(8):777–783. [PubMed: 17646877]

Okumura T, Nagai F, Yamamoto S, Oomura H, Inouye K, Ito M, Sawada H. J Virol Methods. 2005; 124(1-2):143–148. [PubMed: 15664062]

Sakti SP, Rosler S, Lucklum R, Hauptmann P, Buhling F, Ansorge S. Sensors and Actuators A-Physical. 1999; 76(1-3):98–102.

Shen Z, Shih WY, Shih W-H. Appl Phys Lett. 2006; 89:023506–08.

Shih WY, Luo H, Li H, Martorano C, Shih WH. Appl Phys Lett. 2006; 89:242913.

Shih WY, Zhu Q, Shih W-H. J Appl Phys. 2008; 104:074503.

Takahashi Y, Itami T, Maeda M, Suzuki N, Kasornchandra J, Supamattaya K, Khongpradit R, Boonyaratpalin S, Kondo M, Kawai K, Kusuda R, Hirono I, Aoki T. J Fish Dis. 1996; 19:399–403.

Tremont R, De Jesus-Cardona H, Garcia-Orozco J, Castro RJ, Cabrera CR. J Appl Electrochem. 2000; 30(6):737–743.

Tsai JM, Wang HC, Leu JH, Hsiao HH, Wang AH, Kou GH, Lo CF. J Virol. 2004; 78:11360–11370. [PubMed: 15452257]

Wang CH, Lo CF, Leu JH, Chou CM, Yeh PY, Chou HY, Tung MC, Chang CF, Su MS, Kou GH. Dis Aquat Org. 1995; 23:239–242.

Wang CS, Tang KFJ, Kou GH, Chen SN. J Fish Dis. 1997; 20:323–331.

Wang YC, Lo CF, Chang PS, Kou GH. Aquaculture. 1998; 164(1-4):221–231.

Wang HC, Wang HC, Leu JH, Kou GH, Wang AH, Lo CF. Dev Comp Immunol. 2007; 31:672–686. [PubMed: 17188354]

Wongteerasupaya C, Vickers JE, Sriuairatana S, Nash GL, Akarajamorn A, Boonsaeng V, Panyim S, Tassanakajon A, Withyachumnarnkul B, Flegel TW. Dis Aquat Org. 1995; 21:9–77.

Xie X, Li H, Xu L, Yang F. Virus Res. 2005; 108(1-2):63–67. [PubMed: 15681056]

Yi JW, Shih WY, Shih W-H. J Appl Phys. 2002; 91(3):1680–1686.

Yi JW, Shih WY, Shih W-H, Mutharasan R. J Appl Phys. 2003; 93:619–625.

Zhou Q, Qi YP, Yang F. J Virol Methods. 2007; 146(1-2):288–92. [PubMed: 17767964]

Zhu Q, Shih WY, Shih W-H. Biosensors & Bioelectronics. 2007a; 22(12):3132–3138. [PubMed: 17387007]

Zhu Q, Shih WY, Shih W-H. Sensors and Actuators B-Chemical. 2007b; 125(2):379–388.

Zhu Q, Shih WY, Shih W-H. Appl Phys Lett. 2008a; 92:033503.

Zhu Q, Shih WY, Shih W-H. Appl Phys Lett. 2008b; 92:183505–07. [PubMed: 19479043]

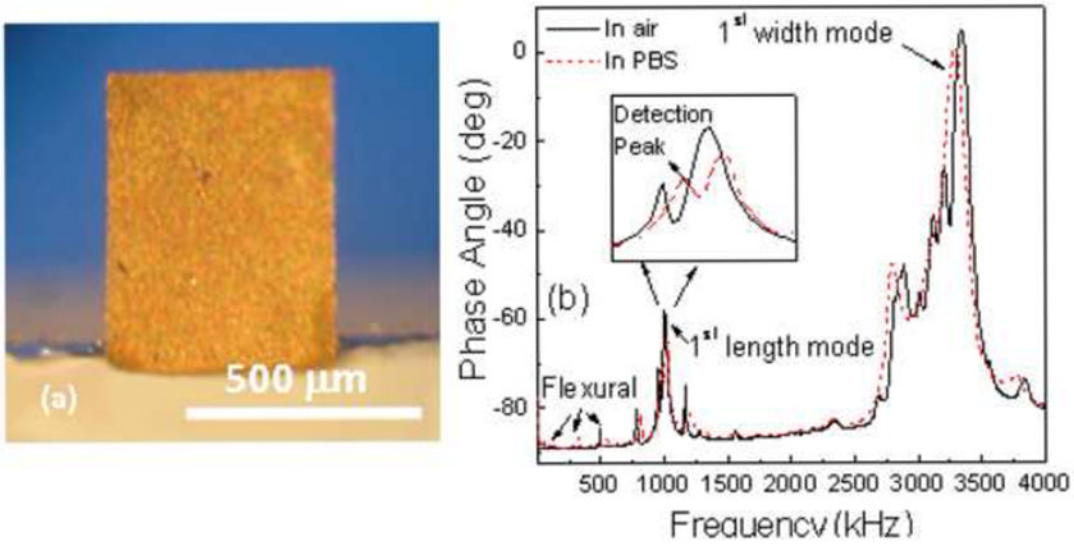

Fig. 1.

(a) An optical micrograph of a 715 μm long and 485 μm wide PMN-PT PEMS viewed from the gold side and (b) a typical phase angle versus frequency resonance spectra of a PMN-PT PEMS in air and in PBS. The detection was carried out with the first longitudinal peak.

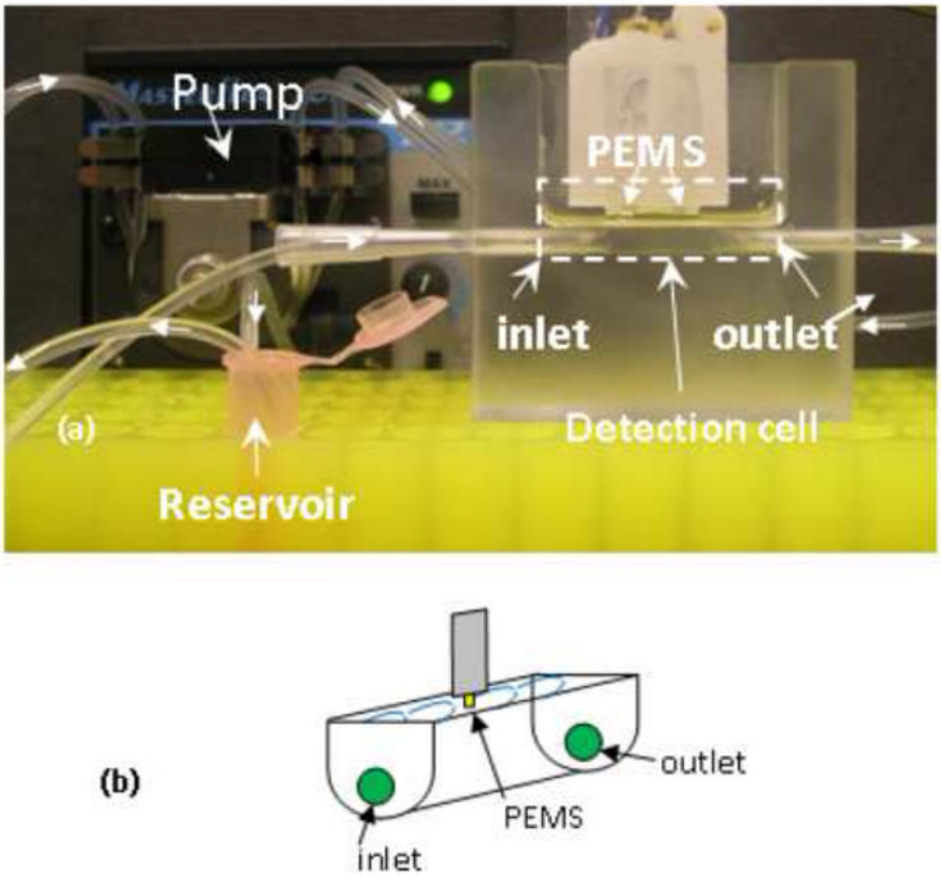

Fig. 2.

(a) A photograph of the flow system consisted of an polycarbonate open detection cell indicated by the dashed rectangle, a reservoir (the pink PCR tube), a peristaltic pump connected with tubes of a 1.5 mm inner diameter, and (b) a schematic of the detection chamber. Both the inlet and the outlet of the detection cell were located near the bottom of the cell while the PEMS were situated near the top of the detection cell and at the center of the flow cell with the major faces of the PEMS parallel to the flow. Both the inlet and outlet tubes were over 1 m long such that the tubes and the reservoir together accounted for most of the 6 ml of liquid volume. The arrows along the tubing indicate the direction of the flow.

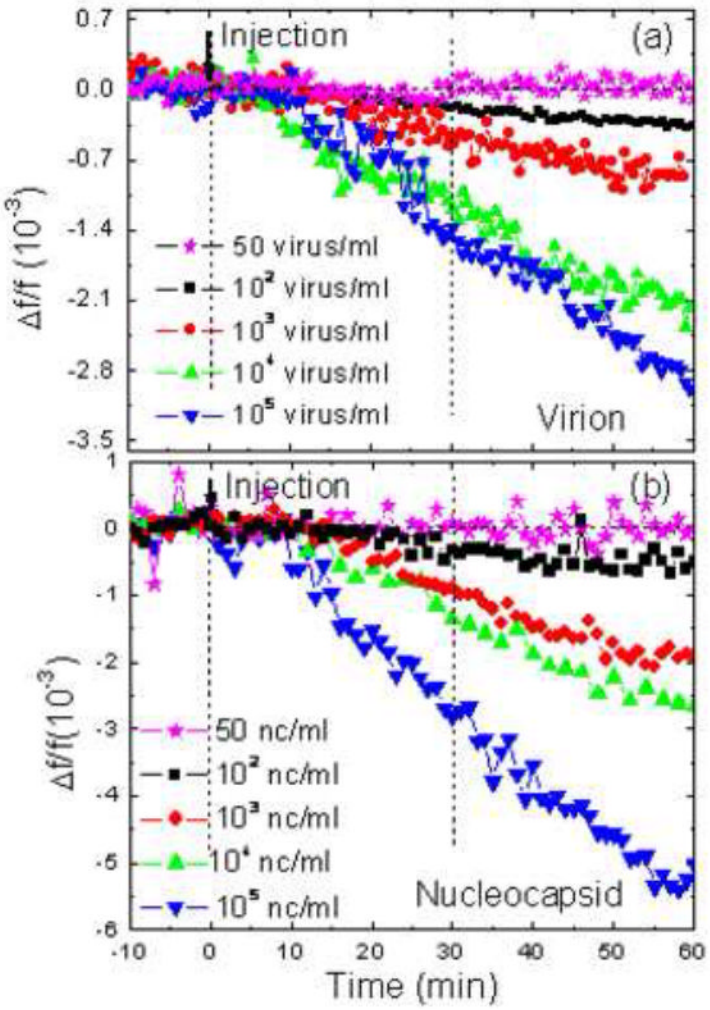

Fig. 3.

Δf/f versus time for (a) virion detection at various virion concentrations and (b) for nucleocapsid detection at various nucleocapsid concentrations.

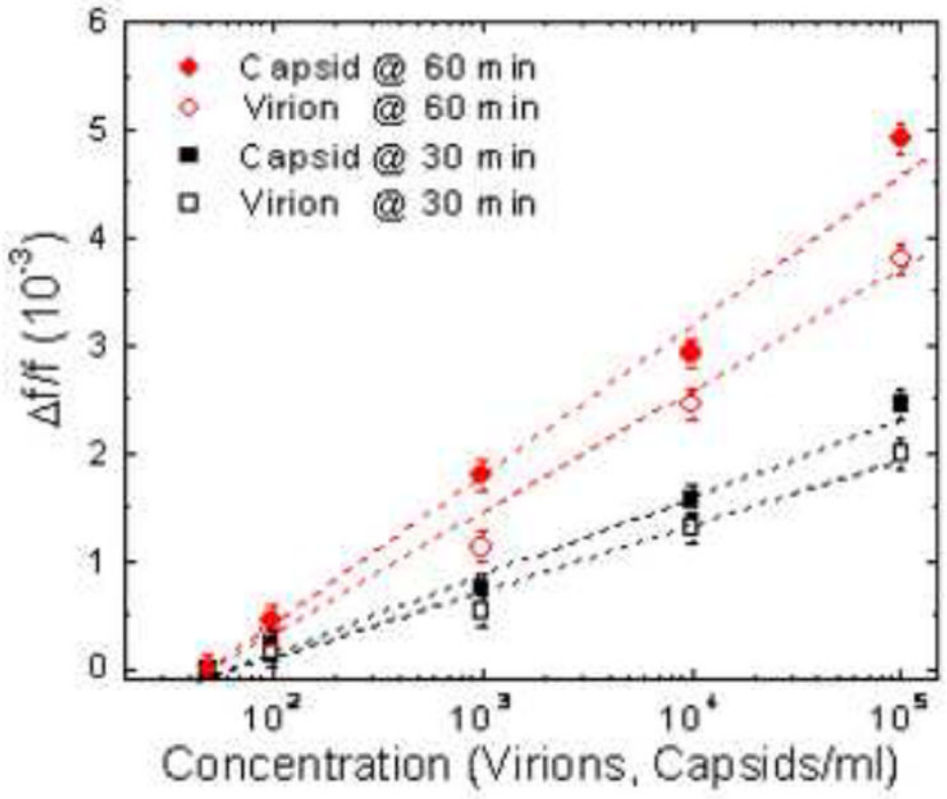

Fig. 4.
Δf/f versus concentration for virion and nucleocapsid detection at time = 30 and 60 min.

Table I

Detection data of the whole virus particles at concentrations ranging from 10^5 to 50 virus/ml. where f was the initial resonance frequency, Δf_{30} and Δf_{60} were the resonance frequency shift averaged over t = 29-31 min and that averaged over t = 55-60 min, respectively. Note that for each Δf and $\Delta f/f$, the numbers after the "±" indicated the noise (half bandwidth) of Δf and $\Delta f/f$ with time, respectively

Virus concentration (virus/ml)	f (kHz)	$-\Delta f_{30}$ (kHz)	$-\Delta f_{60}$ (kHz)	$-\Delta f_{30}/f$ (10^{-3})	$-\Delta f_{60}/f$ (10^{-3})
10^5	660	1.5±0.07	2.6±0.1	2.3±0.1	3.9±0.15
10^4	843	0.94±0.07	1.9±0.1	1.1±0.08	2.25±0.1
10^3	834	0.41±0.07	0.73±0.07	0.5±0.08	0.9±0.08
10^2	774	0.13±0.07	0.28±0.07	0.17±0.08	0.36±0.08
50	788	0±0.07	0±0.07	0±0.08	0±0.08

Table II

Detection data of the nucleocapsid particles at concentrations ranging from 10^5 to 50 virus/ml where f was the initial resonance frequency, Δf_{30} and Δf_{60} were the resonance frequency shift averaged over t = 29-31 min and that averaged over t = 55-60 min, respectively. Note that for each Δf and $\Delta f/f$, the numbers after the "±" indicated the noise (half bandwidth) of Δf and $\Delta f/f$ with time, respectively.

Nucleocapsid concentration (virions/ml)	f (kHz)	$-\Delta f_{30}$ (kHz)	$-\Delta f_{60}$ (kHz)	$-\Delta f_{30}/f$ (10^{-3})	$-\Delta f_{60}/f$ (10^{-3})
10^5	650	1.6±0. 1	3.4±0.1	2.46±0.15	5.23±0.15
10^4	640	1±0.07	1.7±0.07	1.56±0.1	2.66±0.1
10^3	650	0.41±0.06	1.2±0.07	0.63±0.08	1.85±0.1
10^2	655	0.15±0.06	0.3±0.06	0.23±0.08	0.45±0.08
50	665	0±0.06	0±0.06	0±0.08	0±0.08

Table III

Comparison of $\Delta f_{60}/f$ between virion detection and nucleocapsid detection.

Virus concentration (virus/ml)	$-\Delta f_{60}/f$ (10^{-3}) for virion	$-\Delta f_{60}/f$ (10^{-3}) for nucleocapsid
10^5	3.9±0.15	5.23±0.15
10^4	2.2±0.1	2.7±0.11
10^3	0.9±0.1	1.85±0.1
10^2	0.36±0.06	0.45±0.06
50	0±0.05	0±0.075